

Cite this: *Soft Matter*, 2012, **8**, 2452

www.rsc.org/softmatter

PAPER

# Self-assembly of alkoxy-silanized humic substances into multidomain adlayers at the water–solid interface: linking surface morphology to the molecular structure of the adsorbate†

Leonid A. Karpouk,<sup>a</sup> Sergey A. Ponomarenko,<sup>b</sup> Ahmed Mourran,<sup>c</sup> Dmitry Bochkariov,<sup>d</sup> Aziz M. Muzafarov,<sup>b</sup> Kirk Hatfield<sup>e</sup> and Irina V. Perminova<sup>\*a</sup>

Received 18th August 2011, Accepted 6th December 2011

DOI: 10.1039/c2sm06582g

Self assembly of natural organic materials (*e.g.*, humic substances) on mineral surfaces leads to the formation of adlayers with physically different domains. However, direct evidence to explain the molecular interactions responsible for the formation of these domains is still missing. Here, we developed alkoxy-silanized humic probes capable of self-assembling onto hydroxylated surfaces. Using modified humic substances from vastly differed sources (peat, water, coal) and DNA array glass slides as a flat surrogate for mineral surfaces, we create humic adlayers under aqueous conditions and show them to be homogeneous on the macroscale, but consisted of nanosize domains in coal and water humics and submicron-size domains in peat humics. The surface charge and hydrophilic–lipophilic balance of humic associates were proposed as major molecular drivers of the self-assembly with the former causing the formation of thin adlayers composed of separated nanosize domains (*e.g.*, coal humics) and the latter enhancing the formation of thicker adlayers composed of interconnected domains linked in chains up to the submicron-size (*e.g.*, peat humic materials). To the best of our knowledge, this is the first time alkoxy-silanized humic probes were used to examine how humic adsorbates and their molecular structure influences the surface morphology of assembled adlayers. In this fashion, the humic adlayer with molecularly-defined functional elements can be assembled on any hydroxylated surface *in situ*, at the water–solid interface.

## Introduction

Self-assembly of natural organic materials, *e.g.*, humic substances, at the water–solid interface produces organic adlayers on mineral surfaces with structures spanning multiple length scales.<sup>1–5</sup> The chemical–physical properties of these adlayers are of pertinence in aqueous environments, because they strongly influence the stability of suspended colloids and the transport of colloids and contaminants through aqueous environments.<sup>6–9</sup> Numerous sorption studies offer ambiguous results as to how multiple molecular structures, associated with the

humic adsorbates, govern adlayer interactions with hydrophobic organic chemicals: in some studies aromatic moieties are found to be important,<sup>10–12</sup> whereas others advocate the salient role of aliphatic compartments of humic assemblies.<sup>13–16</sup> To explain this disparity, multi-domain sorption models are typically assumed: these models imply the coexistence of expanded (rubbery) and condensed (glassy) regions within the humic adlayer and in turn emphasize the importance of surface morphology over the chemical nature of adlayer compartments.<sup>17–20</sup>

Multiple efforts have since followed to estimate the environmental significance and effects of surface morphologies in humic adlayers. For this purpose, humic substances with different mass fractions of aliphatic and aromatic moieties were covalently bound to a porous silica gel which was functionalized with amino- or epoxy-organosilanes.<sup>21–30</sup> With limited success, it was then feasible to study the interactions between different contaminants and distinct samples of humic-coated silica gels; however, quantification of surface components was ambiguous, and the application of surface specific methods was difficult. To overcome these limitations, an approach was taken to attach humic adlayers to atomic-flat Si-wafers modified with organosilane spacers.<sup>31</sup> The technique required multistage pretreatment of the Si-wafer to covalently attach the aminoorganosilane

<sup>a</sup>Department of Chemistry, Lomonosov Moscow State University, Moscow, 119991, Russia. E-mail: iperm@org.chem.msu.ru; Fax: +7 (495) 9395546; Tel: +7 (495) 9395546

<sup>b</sup>Institute of Synthetic Polymer Materials, Russian Academy of Sciences, Moscow, 117393, Russia

<sup>c</sup>DWI an der RWTH Aachen e.V. and Institute of Technical and Macromolecular Chemistry at RWTH Aachen, Pauwelsstr 8, D-52056 Aachen, Germany

<sup>d</sup>Advantia Inc, Menlo Park, CA, 94025, USA

<sup>e</sup>Department of Civil and Coastal Engineering, University of Florida, Gainesville, FL, 32611, USA

† Electronic supplementary information (ESI) available. See DOI: 10.1039/c2sm06582g

monolayer followed by diazotization to immobilize humic acids. However, this approach cannot be used to model the process of *in situ* self-assembly of a humic adlayer at the water–solid interface. As a result, direct experimental evidence remains to be gathered on the molecular interactions which drive self assembly of humic substances into adlayers of certain morphologies. Elucidating the driving force behind these interactions would enable substantial progress to be made using humic adsorbates to engineer reactive surfaces in aqueous environments, such as with the *in situ* installation of permeable reactive barriers in the contaminated aquifers by guided self assembly of humic adlayers on mineral surfaces, or with the *in situ* synthesis of stable nanoparticles in aqueous solutions using humic substances as efficient macrologands.

The goal of this study was to define the major molecular drivers of self assembly of humic substances into adlayers of the specific nanomorphologies at the water–solid interface. To achieve this goal, the following objectives were formulated: (1) to develop a simple, one-step method for engendering guided self-assembly of humic adlayers from aqueous solutions on oxidized silicon supports, (2) to test the performance of the method using humic substances with substantially different molecular properties and flat surrogates of mineral surfaces, (3) to investigate the morphology of created adlayers at the nanoscale using surface specific methods, (4) to establish a link between monolayer morphologies and specific molecular compositions of humic adsorbates.

To achieve these objectives, we developed a novel approach that gives rise to the self-assembly of humic substances into adlayers at the water–solid interface as schematically shown in Fig. 1.

The surface chemistry of humic substances is modified by reacting carboxyl and hydroxyl groups of humic polyanions with amino and epoxy groups of 3-amino- and 3-glycidoxy-propyltrimethoxysilanes, respectively. Trimethoxysilyl groups are then incorporated into the humic backbone, where they serve as spacers to covalently bind the humic adlayer to mineral surfaces. Used in this study is a set of well characterized humic materials from vastly different natural sources (coal, peat, water). Each sample differs with respect to surface charge, molecular weight, and hydrophilic–lipophilic balances. DNA array glass slides serve as flat surrogates of mineral surfaces suitable for studies with a use of surface specific methods. Confocal laser scanning microscopy (CLSM) and scanning force microscopy (SFM) are used for this purpose. The major molecular drivers of self assembly of humic adlayers at the water–solid interface are

identified. Promising applications of the guided self-assembly of humic adsorbates in nanoremediation are discussed.

## Experimental section

### Synthesis of humic molecular probes with mineral adhesive sites

Humic materials used for modification were isolated from vastly different natural sources (coal, peat, fresh water). Commercially available potassium humate from oxidized coal, leonardite (Powhumus; Humintech Ltd., Germany), low moor peat from the Tver region (Russia), and water from the River Istra (Moscow District, Russia) served as the sources of humic materials. The isolation procedures were based on the corresponding protocols of the International Humic Substances Society.<sup>32</sup> The isolated humic materials represented humic acid fraction from coal (CHP), humic acid fraction from peat (PHS), and non-fractionated humic material from fresh water (AHS).

The alkoxylation of the humic materials was conducted using 3-aminopropyltrimethoxysilane (APTS) and 3-glycidoxypropyltrimethoxysilane (GPTS). All the humic materials were dehydrated using azeotropic distillation with dry toluene, mixed with dry dimethylformamide (DMF) and reacted with the APTS under continuous stirring for 20 h at 120 °C. The DMF was rotary-evaporated, the reaction product was dried at 40 °C for 4 h and stored in a desiccator. For all humic materials the reaction was run at 1 : 1 reagent molar ratio which equalled 1.0 g of APTS per 1.0 g of humic material. For CHP, it was also run at 0.2 g of APTS per g of CHP. The corresponding amounts of APTS were calculated on the basis of COOH groups present in the humic sample (*e.g.*, 3.8 mmol per g for CHP).

Modification using GPTS was conducted with coal humic acids (CHP). GPTS (1.1 mL) was added to a suspension of 1 g of dry CHP in dry CH<sub>2</sub>Cl<sub>2</sub> and then few drops of CF<sub>3</sub>SO<sub>3</sub>H were added at –15 °C. The reaction was carried out for 10 h under argon atmosphere. CH<sub>2</sub>Cl<sub>2</sub> was evaporated and the resulting product dried at 40 °C, and stored in a desiccator. The prepared alkoxylation humic materials were from dark brown to black in color which was similar to the color of the parental material.

### Characterization of the modified humic materials

All parental and modified humic materials were characterized using elemental analyses (C, H, N) performed on a Carlo Erba Strumentazione analyzer. The Si content was determined using Specord M40. Acidic group analyses were carried out as described elsewhere<sup>32</sup> using barium hydroxide and calcium

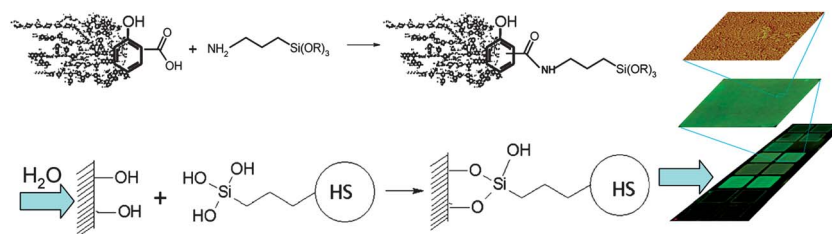


**Fig. 1** Schematic reaction pathway for alkoxylation of humic substances (upper reaction scheme) and their guided self-assembly at the water–solid interface on glass surfaces (bottom reaction scheme) with formation of adlayers: homogeneous at macroscale (green patch: fluorescence image) and heterogeneous at nanoscale (upper patch: scanning force microscopy (SFM) image).

acetate techniques for determination of total and carboxylic acidity, respectively. Molecular weight distribution was studied using Size Exclusion Chromatography (SEC) as described in ref. 33. For this purpose, a liquid chromatography system consisted of a solvent pump (Abimed), a packed column, and a UV-VIS detector with variable wavelength was used. The UV-absorbance was measured at 254 nm. The SEC column was 25 × 200 mm packed with Toyopearl HW-55S. Phosphate buffer (0.028 M, pH 6.8) was used as the mobile phase at a flow rate of 1 mL min<sup>-1</sup>. A sample of HS for SEC analysis was dissolved in the minimum amount of NaOH and diluted to the concentration of 100 mg L<sup>-1</sup> with a buffer solution used as the mobile phase. 1 mL volume of this solution was injected for analysis. The SEC column was calibrated using sodium polystyrenesulfonates (PSS), kDa: 14.0; 20.7; 45.1; and 80.84. The standard kits were purchased from the Polymer Standard Service (Mainz). Blue dextran (2000 kDa) served as a void volume probe, and acetone as a permeation volume probe. The results on elemental and functional analyses and molecular weight characteristics are shown in Table 1.

A comparison of original humic substances shows aliphatic fractions, indicated by the H/C ratio, and acidic groups were substantially higher in materials from water and peat than from coal. Molecular weights of aquatic and coal materials were much lower than those for the peat materials. In the alkoxy-silanized humic materials, the silicon content indicating the amount of incorporated APTS increased in accordance with the carboxylic acidity of the parent humic sample (e.g., CHP-APTS-100 < PHS-APTS-100 < AHS-APTS-100). For the alkoxy-silanized humic materials from coal (CHP-APTS-20 and CHP-APTS-100), the silicon content increased as expected with the APTS to CHP molar ratio. With respect to the GPTS-humic material (CHP-GPTS-100), an expected decrease in phenolic group content was observed; confirming the reaction with the epoxy ring of GPTS.

### <sup>13</sup>C NMR spectroscopy

Quantification of aromatic and aliphatic units was conducted using <sup>13</sup>C NMR spectroscopy. <sup>13</sup>C solution-state NMR spectra were acquired on solutions of humic materials in 0.3 M NaOD at a concentration of 100 g L<sup>-1</sup> using a 5 mm broadband observe probe head on a Bruker AC 400 (Rheinstetten, Germany) spectrometer operating at 100.62 MHz for <sup>13</sup>C, using inverse gate decoupling, a single spin-echo sequence (delay 10 μs) and an interpulse delay of 8 s (acquisition time: 229 ms for parental humic materials and 917 ms for selected modified derivatives; 90-

deg (<sup>13</sup>C): 8,6 s; *T* = 303 K; SW = 71428 Hz). These conditions have been previously shown to provide quantitative determination of carbon distribution among the main structural fragments of HS.<sup>33</sup> Section integrals were attributed as follows<sup>34</sup> (in ppm): 5–50, aliphatic non-substituted C atoms (C<sub>Alk</sub>); 50–108, aliphatic O-substituted C atoms (C<sub>Alk-O</sub>); 108–145, aromatic non-substituted C atoms (C<sub>Ar-H,C</sub>); 145–165, aromatic O-substituted C-atoms (C<sub>Ar-O</sub>); 165–187, C atoms of carboxylic and ester groups (C<sub>COO</sub>); and 187–220, C atoms of quinonic and ketonic groups (C<sub>C=O</sub>).

### Fabrication of humic adlayers on glass surfaces

For self-assembly of alkoxy-silanized humic materials on glass surfaces, two microscope glass slides were used of Borofloat (Schott Nexterion). These glass slides are specifically manufactured to suit DNA arrays with minimum surface roughness. The glass surface was activated using the procedure described in ref. 35. The purpose of the treatment was to etch the glass and promote attachment of silanol groups. In brief, the slides were heated at 260 °C for 8 h and left in the oven to cool overnight. Next, the slides were washed with 10% NaOH dissolved in 40% EtOH for 2 h on orbital shaker at 90 rpm. The slides were then washed with water 4 times, for 5 min each. The pH of the last water wash was 7.1. As a final step, the slides were washed with EtOH for 5 min on an orbital shaker, 90 rpm, quickly transferred to a dry container with 6 layers of particle-free wipe pads (DRUX-70) and spun down vertically along the long axis at 2000 rpm for 4 min at 20 °C in a 216 rotor (IEC) with slide containers placed directly into the regular buckets. A plastic structure was attached to the slides to create 16 square isolated compartments so that multiple humic materials could be applied to the surface of the same slide. Six samples of humic materials were used for assembly onto the glass surface, nominally, CHP-APTS-20, CHP-APTS-20 (heated), PHS-APTS-100, CHP-APTS-100, AHS-APTS-100 and CHP-GPTS-100. Non-modified humic acids from coal (CHP) was used as a control. The alkoxy-silanized humic materials were applied on dry surfaces as solutions in phosphate buffer (0.028 M, pH 6.8) at concentrations of 1 g L<sup>-1</sup>. The prepared glass slides were left overnight, then rinsed with distilled water and dried.

### Confocal laser scanning microscopy

The surfaces of glass slides with self assembled adlayers of humic materials were scanned using a high resolution confocal dual-laser

**Table 1** Structural and molecular weight characteristics of the original and silanized humic materials

| Sample       | Silicon content (% mass), atomic ratios, and content of acidic groups (mmol g <sup>-1</sup> ) |      |       |             |      | <i>M</i> <sub>w</sub> , kDa | <i>M</i> <sub>w</sub> / <i>M</i> <sub>n</sub> |
|--------------|---|------|-------|-------------|------|-----------------------------|---|
|              | Si  | H/C  | N/C   | COOH        | ArOH |                             |   |
| PHS          | n.d.  | 1.08 | 0.055 | 4.2 ± 0.1   | 1.5  | 11.1                        | 3.2   |
| PHS-APTS-100 | 11.4  | 1.55 | 0.192 | 0.09 ± 0.01 | 0.9  | 12.3                        | 2.3   |
| AHS          | 1.26  | 1.05 | 0.041 | 5.4 ± 0.1   | 1.1  | 5.5                         | 2.0   |
| AHS-APTS-100 | 13.2  | 1.35 | 0.155 | 0.07 ± 0.01 | 0.2  | 6.9                         | 2.1   |
| CHP          | 2.11  | 0.87 | 0.018 | 3.8 ± 0.1   | 1.8  | 6.0                         | 3.3   |
| CHP-APTS-20  | 4.22  | 1.12 | 0.089 | 1.09 ± 0.1  | 1.7  | 8.6                         | 5.0   |
| CHP-APTS-100 | 7.02  | 1.45 | 0.094 | 0.41 ± 0.01 | 1.1  | 9.7                         | 3.9   |
| CHP-GPTS-100 | 6.75  | 1.11 | 0.022 | 3.8 ± 0.1   | 1.4  | 8.1                         | 3.6   |

fluorescence microarray scanner, AlphaScan (Alpha Innotech corporation/CapitalBio corporation) in two channels: at excitation wavelength of 532 nm and 635 nm and respective emission wavelengths, 570–590 nm and 680–700 nm. For graphical representation purposes, a green color was assigned to the 532 nm laser channel and a red color to the 635 nm channel.

### SFM studies

The morphology of the humic adlayers on the glass slides was investigated by scanning force microscopy (SFM) at room temperature with a Nanoscope IIIa controller. The imaging was done in the tapping mode using standard silicon cantilevers (Nanoworld Pointprobe) with a nominal resonance frequency of 75 kHz. The preparation of the glass surfaces is well described in the previous section and the surface of a floated-glass (Borofloat) is appropriate for SFM investigations.

The height images were analyzed by considering the root mean square roughness (RMS) and the distribution of height which differentiates the relief of the surface from its roughness. For consistent comparison the evaluation was performed over  $3 \times 3 \mu\text{m}^2$  and  $1 \times 1 \mu\text{m}^2$  surface areas. Note that featureless smooth surfaces have a Gaussian height distribution with half width maxima equal to the surface roughness. Thus, adsorption of material to glass surfaces generates additional surface relief and alters the surface distribution which we consider as a measure of surface coverage.

## Results and discussion

The most important feature of the synthesized alkoxy-silanized humic substances was solubility in aqueous alkali solutions accompanied with hydrolysis of alkoxy-silyl groups to silanols capable of producing siloxane bonds with surfaces of silicon oxides, *e.g.* glass. Covalent bonding is of particular importance as it precludes the facile mobilization of the humic adlayer and facilitates the use of surface specific methods. This made them perfect surface probes for guided self assembly of humic adlayers on surfaces of oxidized silicon substrates (*e.g.* glass slides) aimed at mimicking geochemical interfaces in natural soil or sediment systems.

The self assembled humic adlayers on the surfaces of the glass slides were visualized using confocal laser fluorescence scanning microscopy with the scan resolution of  $5 \mu\text{m}$  and SFM. The combined use of the above techniques enables coverage of a wide spatial scale from macro/meso to micro/nano-levels. Application of alkoxy-silanized humic probes to DNA array glass slides and imaging results for fluorescence microscopy are shown in Fig. 2.

The fluorescence images of humic adlayers on two glass slides treated with the same humic materials under consistent conditions are similar and indicative of good reproducibility in the self-assembly approach. Glass surfaces with attached humic adlayers differed substantially from those exposed to phosphate buffer or to a solution of non-modified humic materials. The highest fluorescence intensities were observed for surfaces treated with alkoxy-silanized peat humic acids (PHS-APTS-100) and aquatic humic materials (AHS-APTS-100) which may be an indicator of adlayer thickness or the amount of the attached humic material. The level of fluorescence intensity indicates that the peat humic

probes produced the thickest layers. A comparison of image color intensities shows the greenest images, indicating fluorescence emissions in the high 500s, were observed for aquatic humic materials; whereas, the reddish color, characteristic of fluorescence emissions in the high 600s, were observed for CHP-APTS-100. Yellow color (a superimposed mix of green and red) was observed for peat materials indicating fluorescence in both channels. Results corroborate the fluorescence properties of humic materials with the shortest emission maxima characteristic of low molecular weight aquatic humics and the much longer wavelength characteristics of the emission maxima of aromatic-rich coal humics.<sup>36</sup>

Of particular interest is the absence of fluorescence from surfaces treated with GPTS-silanized humic materials and parental humic material from coal (two bottom rows in Fig. 2). This is an indication that GPTS treated material from coal had less affinity for binding to glass surface than humics treated with APTS. This is consistent with the higher surface charge of GPTS-material (carboxylic acidity of  $3.8 \text{ mmol g}^{-1}$ ) as compared to the APTS-treated coal materials (Table 1). Non-modified humic materials, as expected, did not attach to glass due to a lack of positively charged vacancies at the water–solid interface which drives their interaction with aluminosilicates in nature. The function of positive vacancies was successfully reproduced in this study with the incorporation of the anchoring alkoxy-silyl groups in the humic structure. In general, results show complete coverage of glass surfaces with self-assembled layers of the APTS-treated humic materials from different sources which looked rather homogeneous at a resolution of  $5 \mu\text{m}$ .

To further assess the homogeneity of adlayers, glass slides were imaged with SFM. Fig. 3 shows the surface topography of the three samples—coal, peat and aquatic humic materials—with corresponding height distributions.

The SFM results show that all the humic adlayers have thicknesses of few nanometres consisting of globular-like adsorbates. Substantial differences can be seen between the surface coverage depending on the source of the humic materials (coal, peat, water). Surface features varied from predominantly flat (coal), to elevated (peat), and to flat again with isolated clumps (water). Hence, the source of parental humic material defines surface morphology of the adlayer including relief, surface coverage, and roughness.

Indeed, coating based on modified coal humic acids (Fig. 3a) shows an rms-roughness (RMS) of about 1.5 nm and a symmetric height distribution with half width maximum of about 3 nm. In contrast, coatings prepared from peat (Fig. 3b) or aquatic humic acids (Fig. 3c) are somewhat rougher with an RMS of about 4–6 nm, and asymmetric height distributions, extending to heights of about 10 nm which exceed the surface roughness. This suggests APTS modified coal humic materials generate a chemisorbed adlayer with a lower surface density than that of peat or aquatic materials. This is in agreement with fluorescence microscopy where a corresponding coal-based coating (CHP-APTS-100) exhibits much lower fluorescence intensity as compared to peat and water materials.

In principle, adlayer formation by chemisorption requires first physical adsorption and subsequent covalent attachment of alkoxy-silanized humic materials to the glass surface. Because non-modified humic materials do not adsorb, this suggests interactions

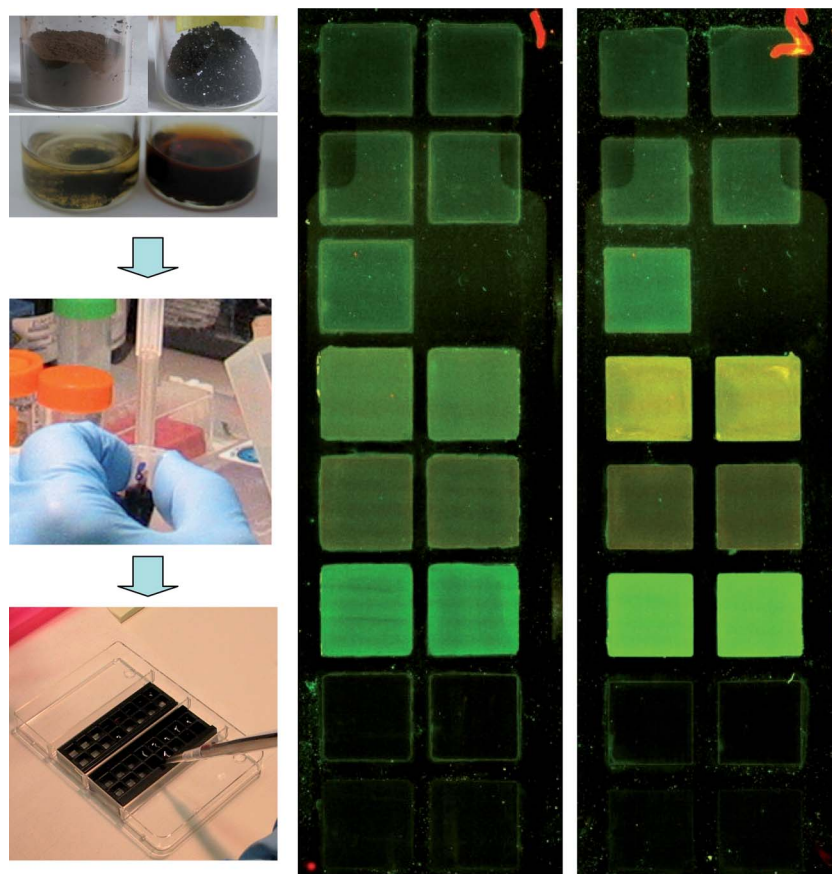


**Fig. 2** General view of the alkoxyfunctionalized humic probes in solid and dissolved state applied to the surface of the DNA array glass slides segregated into multiple patches by the plastic chamber (left part) and the “artificial” color images of the humic adlayers self assembled *in situ* at the water–solid interface (right part). Left upper image shows four glass beakers with solid and dissolved humic probes made from coal (dark color) and peat (light color) humic materials. The middle left image shows pipetting, and the bottom image shows the application of humic probe solutions to the surface of glass slides. The right side shows fluorescence images of duplicate glass slides treated with the same humic materials. The slides were scanned in a laser microarray scanner in two channels: Ex. 532 nm; em. 570–590 nm (green); Ex. 635 nm; em. 680–700 nm (red). The samples, listed bottom to top, are as follows: the bottom (first) row is a parental coal humics (CHP), the second row is CHP-GPTS-100, the third row is AHS-APTS-100, the fourth row is CHP-APTS-100, the fifth row is PHA-APTS-100, the sixth row is buffer solution (right side, the background control) and CHP-APTS-20-non-heated (left side), the seventh row is CHP-APTS-20 non-heated, the eighth row is CHP-APTS-20 (heated).

in the vicinity of glass surfaces are essentially repulsive. This is most likely due to the surface charge of glass and humic acid, both of which are negative according to the near neutral pH (6.8) and low ionic strength ( $0.044 \text{ mol L}^{-1}$ ) of the aqueous medium. Yet, introducing APTS reactive groups overcomes surface repulsion and enables permanent bonding of the humic materials to the glass surface. Thus, adhesive interactions are governed by affinity of the silanol groups, which anchor to hydroxyl groups at the glass surface. Repulsive interactions are electrostatic in origin; they vary with the surface charge of glass and the molecular mass and charge of the adsorbate. Chemisorption can be most effective when reactive groups bind cooperatively. Such was the case for the APTS modified humic materials, where an elevated number of reactive end-groups produced a dense adlayer. The incorporated trisilanol end-groups drove the attachment of humic associates to the glass surface through formation of siloxane bonds, and they invoked lateral condensation of the adlayer which could be further enhanced or prevented by the intermolecular interactions discussed below.

Qualitatively, the molecular weight of native or APTS modified AHS and CHP are similar; however, they essentially differ in the content of incorporated silicon. Humic materials, from aquatic sources, acquired two-times more Si after modification than those from coal (see Table 1). Assuming the Si content was proportional to the number of incorporated functional groups per molecule, this would suggest that aquatic humic acids form a much denser adlayer than coal. This is in agreement with the SFM observations. In the cases of PHS-APTS and AHS-APTS, both humic materials contain similar amounts of Si, but the molecular mass of peat is much higher; hence, there is a lower density of silanol groups per molecule of PHS-APTS as compared to that of AHS-APTS. Still, peat humic acids produced a surface coverage higher than that of aquatic humics as probed by SFM. The explanation could be additional cooperative interactions contributed by a favorable hydrophilic–lipophilic balance of peat materials.

To prove this assumption, we have estimated the hydrophilic–lipophilic balance of the humic materials using  $^{13}\text{C}$  NMR

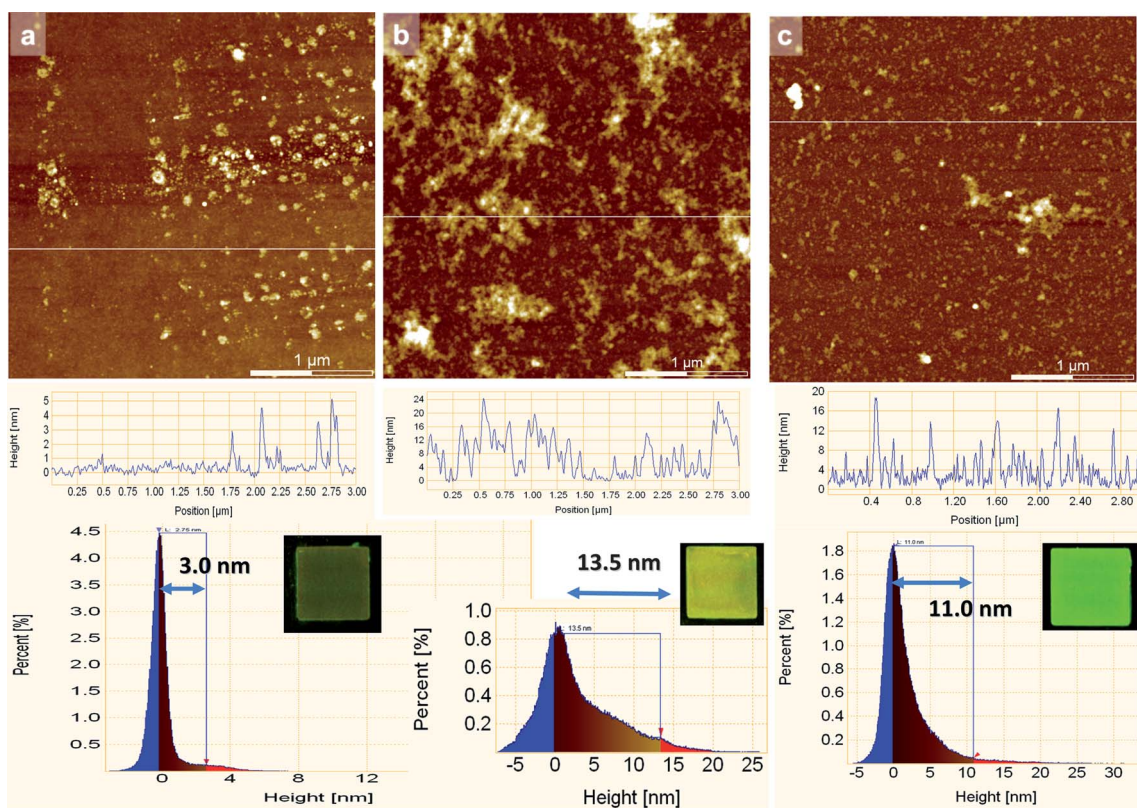


**Fig. 3** Height SFM images of the glass surfaces modified with the alkoxy-silanized humic substances from different sources. (a) CHP-APTS-100-treated surface with an RMS roughness of about 1.5 nm. (b) PHS-APTS-100-treated surface with an RMS roughness of 5.9 nm. (c) AHS-APTS-100-treated surface with an RMS roughness of 3.8 nm. The roughness was determined from  $3 \times 3 \mu\text{m}^2$  surface area. For clarity we also include the fluorescence image of the same sample. The graphs below each image represent a cross section profile along the horizontal line as indicated, and the corresponding height distributions.

data which enable quantitative assessment of carbon distribution among the building blocks of humic molecules (Fig. 4 and Table 2).

From the  $^{13}\text{C}$  NMR data, it is evident that non-modified humic materials differed substantially in carbohydrate carbon content with the maximum value of 24% found in peat, and respective

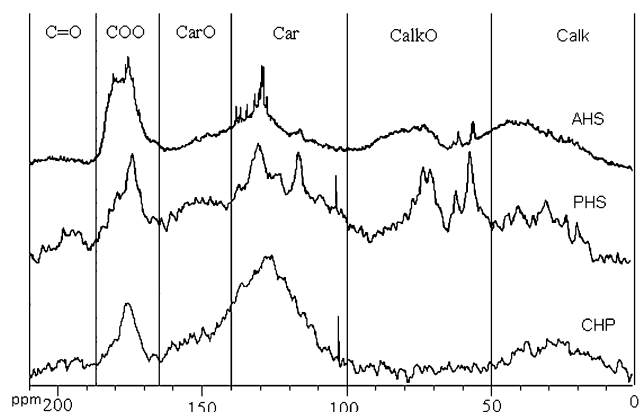


**Fig. 4**  $^{13}\text{C}$  NMR spectra of the parental humic materials—coal humic acids (CHP), peat humic acids (PHS) and aquatic humic substances (AHS). The spectra show essential difference of the humic materials studied in the content of carbohydrates ( $C_{\text{alkO}}$ ) and the content of aromatic structures ( $C_{\text{ar}}$  and  $C_{\text{arO}}$ ).

fractions of 15 and 7% in aquatic and coal humics. In contrast, aromaticity varied in the reverse order reaching 54% for coal humics and decreasing to 35 and 33% for aquatic and peat humic materials respectively. All three materials had essentially the same content of non-substituted aliphatic carbon of alkyl-chains. Data revealed essential interactions of structural features within humic assemblies such as the prevalence of hydrophilic (carbohydrate) moieties over lipophilic (aromatic) moieties. The hydrophilic–lipophilic balance of humic assemblies was quantitatively assessed using the  $C_{\text{alkO}}/\Sigma C_{\text{ar}}$  ratio, where  $C_{\text{alkO}}$  equals the amount of carbon in hydrophilic carbohydrate units, and  $\Sigma C_{\text{ar}} = C_{\text{arO}} + C_{\text{ar}}$  is the amount of carbon in the aromatic rings. Previously we showed this approach to be an effective predictor of polycyclic aromatic hydrocarbon binding affinities to humic materials.<sup>37</sup> From Table 2 it can be deduced  $C_{\text{alkO}}/\Sigma C_{\text{ar}}$  approached 0.73 for peat humics, which was a factor of two higher than aquatic materials and more than five times greater than 0.13 observed for coal. It means that peat humics can be treated as highly hydrophilic materials as compared to aquatic and coal materials.

Estimates of surface charge and hydrophilic–lipophilic balance for alkoxy-silanized humic materials are consistent with trends observed in adlayer morphologies. Coal humic materials, with the highest surface charge and lowest hydrophilicity, were likely to form a diffuse adlayer composed of separated nano-size domains. Whereas, low charged and highly hydrophilic peat

**Table 2** Molecular parameters of the parental humic materials used in this study as determined by  $^{13}\text{C}$  NMR spectroscopy

| Sample | Carbon distribution among structural groups of humic materials, % of C |                         |                        |                          |                         | Ratios of aliphatic to aromatic moieties                 |  |
|--------|--|-------------------------|------------------------|--------------------------|-------------------------|--|--|
|        | $\text{C}_{\text{COO(H/R)}}$   | $\text{C}_{\text{arO}}$ | $\text{C}_{\text{ar}}$ | $\text{C}_{\text{alkO}}$ | $\text{C}_{\text{alk}}$ | $\sum \text{C}_{\text{alk}} / \sum \text{C}_{\text{ar}}$ | $\text{C}_{\text{alkO}} / \sum \text{C}_{\text{ar}}$ |
| CHP    | 16   | 8                       | 46                     | 7                        | 23                      | 0.6  | 0.13   |
| PHS    | 20   | 8                       | 25                     | 24                       | 23                      | 1.4  | 0.73   |
| AHS    | 24   | 11                      | 24                     | 15                       | 26                      | 1.2  | 0.43   |

materials demonstrated the highest affinity for self-assembly at the water–glass interface: these materials produced adlayers composed of interconnected domains of submicron-size. Aquatic materials fell closer to those from peat.

The types of nanostructures described above for the adlayers are in general agreement with the SFM-images observed for the natural humic colloids and for the humic adlayers immobilized onto different mineral surrogates (glass, oxidized silicon wafer, mica, carbonaceous or goethite surfaces).<sup>1–3, 38–42</sup> As in this study, immobilized SRFA and SRHA (IHSS standard humic materials from the Suwannee River) produced adlayers with isolated structures of aquatic humics.<sup>38</sup> Very close estimates of particle shapes and sizes are reported for humic colloids: flat particles (8–13 nm in diameter), aggregates of particles (20–100 nm), chain-like assemblies, networks and torus-like structures.<sup>40</sup> However, we could not find in the literature direct comparison of the structures observed within the adlayers assembled by humic materials from contrasting sources as examined in this study.

Results shed light on processes controlling the surface morphology of adlayers created from natural organic materials. They give complementary explanation of the leading role of aliphatic fragments in formation of glassy (condensed) domains frequently reported in the literature.<sup>12–16, 43</sup> This research was able to elucidate contributions from carbohydrate moieties driving the hydrophilic–lipophilic balance of humic associates during the formation of interconnected domains of submicron-size. This finding can be used to guide the assembly of humic adlayers with desired properties using alkoxy-silanized humic probes manufactured from the humic materials with the appropriate structural features.

## Conclusions

In conclusion, alkoxy-silanized humics can be used as surface probes to study the *in situ* self-assembly of humic adlayers on mineral surfaces at the water–solid interface. Surface activity of natural humic materials was substantially enhanced through incorporation of alkoxy-silyl-moieties that enabled their attachment to glass surfaces. 3-Aminopropyltrimethoxysilane was shown to be much more efficient as compared to 3-glycidoxypropyltrimethoxysilane. A selection of humics from vastly different natural sources (coal, peat, and water) was used to study molecular effects and controls on adlayer assembly. Humic adlayers on glass exhibited homogeneity on the macroscale and considerable multidomain structural heterogeneity on the nanoscale. The roughest and thickest adlayers were acquired with carbohydrate-rich peat humic acids and the thinnest from coal humics with the highest surface charge and hydrophobicity.

The conclusion was made on the important contribution of the hydrophilic–lipophilic balance to adhesive interactions of silanized humic materials attached to the glass surface. To the best of our knowledge, this is the first time that alkoxy-silanized humic probes were used to examine how humic adsorbates and their molecular structure influence the surface morphology of assembled adlayers. Using alkoxy-silanized humic materials with specified structures, we endow humic adlayers with molecularly-defined functional elements.

The discerned relationships between molecular features of humic adsorbates and surface morphologies of the adlayers can be effectively applied for developing new nanoremediation technologies and nanomaterials. For example, the alkoxy-silanized humic materials with high driving force for self-assembly into adlayers at the water–solid interface can be used as active agents in nanoremediation through the *in situ* installation of permeable reactive barriers. This can be achieved by injection of the alkoxy-silanized humic materials into a contaminated aquifer using a fence row of wells. Humic adlayers then self assemble on the mineral surfaces of aquifer materials, where they serve as immobilized zones to intercept and retain metallic and organic contaminants. Another promising field for humics-assisted surface engineering is the *in situ* synthesis of water-stable suspensions of metal-based nanoparticles, *e.g.* magnetic iron oxides. The surface-activated humic materials might serve as effective and biocompatible natural surfactants for synthesis of nanoparticles of new morphologies.

## Acknowledgements

We wish to thank Dr N. Hertkorn (Helmholtz Zentrum Muenchen, Germany) for invaluable help in acquiring NMR spectra. This research was supported by RFBR (grants 10-03-00803, 11-03-12177), US DOE (project RUC2-20006) and NATO-CLG (grant ESP.EAP.CLG 983197).

## References

- 1 P. A. Maurice, in: Mineral-Water Interfacial Reactions, ed.: D. L. Sparks, T. J. Grundl, *ACS Symposium Series*, 1998, 715, p. 57.
- 2 K. Namjesnik-Dejanovic and P. A. Maurice, *Geochim. Cosmochim. Acta*, 2001, **65**, 1047.
- 3 M. Plaschke, J. Roemer, R. Klenze and J. I. Kim, *Colloids Surf., A*, 1999, **160**, 269.
- 4 E. M. Thurman, *Organic geochemistry of natural waters*, ed. M. Nijhof, Dr W. Junk Publishers, Dordrecht, The Netherlands, 1985.
- 5 K. Gosh and M. Schnitzer, *Soil Sci.*, 1982, **129**, 226.
- 6 J. F. McCarthy and J. M. Zachara, *Environ. Sci. Technol.*, 1989, **23**, 496.
- 7 H. v. d. Weerd, A. Leijnse and W. H. Van Riemsdijk, *J. Contam. Hydrol.*, 1998, **32**, 313.
- 8 P. Grathwohl, *Environ. Sci. Technol.*, 1990, **24**, 1687.

- 9 B. Xing and J. J. Pignatello, *Environ. Sci. Technol.*, 1997, **31**, 792.
- 10 Z. Chen, B. Xing, W. B. McGill and M. J. Dudas, *Can. J. Soil Sci.*, 1996, **76**, 513.
- 11 R. Ahmed, R. S. Kookana, A. M. Alston and J. O. Skjemstad, *Environ. Sci. Technol.*, 2001, **35**, 878.
- 12 A. S. Gunasekara and B. Xing, *J. Environ. Qual.*, 2003, **32**, 240.
- 13 M. Khalaf, S. D. Kohl, E. Klumpp, J. Rice and E. Tombacz, *Environ. Sci. Technol.*, 2003, **37**, 2855.
- 14 J. D. Mao, L. Hundal, M. Thompson and K. Schmidt-Rohr, *Environ. Sci. Technol.*, 2002, **36**, 929.
- 15 M. J. Salloum, B. Chefetz and P. G. Hatcher, *Environ. Sci. Technol.*, 2002, **36**, 1953.
- 16 K. W. Fomba, P. Galvosas, U. Roland, J. Kaerger and F.-D. Kopinke, *Environ. Sci. Technol.*, 2011, **45**, 5164.
- 17 W. J. Weber Jr, E. J. LeBoeuf, T. M. Young and W. Huang, *Water Res.*, 2001, **35**, 853.
- 18 M. L. Brusseau, R. E. Jessup and P. S. C. Rao, *Environ. Sci. Technol.*, 1991, **25**, 134.
- 19 W. Huang, M. A. Schlautman and W. J. Weber, *Environ. Sci. Technol.*, 1996, **30**, 2993.
- 20 J. J. Pignatello and B. Xing, *Environ. Sci. Technol.*, 1996, **30**, 1.
- 21 L. K. Koopal, Y. Yang, A. J. Minnaard, P. L. M. Theunissen and W. H. Van Riemsdijk, *Colloids Surf., A*, 1998, **141**, 385.
- 22 G. Szabo, S. L. Prosser and R. A. Bulman, *Chemosphere*, 1990, **21**, 729.
- 23 G. Szabo, S. L. Prosser and R. A. Bulman, *Chemosphere*, 1990, **21**, 777.
- 24 G. Szabo and R. A. Bulman, *J. Liq. Chromatogr.*, 1994, **17**, 2593.
- 25 G. Szabo, G. Farkas and R. A. Bulman, *Chemosphere*, 1992, **24**, 403.
- 26 J. Gucci, A. Angelova, G. Szabo and R. A. Bulman, *React. Polym.*, 1992, **17**, 61.
- 27 A. G. S. Prado, B. S. Miranda and G. V. M. Jacintho, *Surf. Sci.*, 2003, **542**, 276.
- 28 A. G. S. Prado, B. S. Miranda and J. A. Dias, *Colloids Surf., A*, 2004, **242**, 137.
- 29 A. G. S. Prado, J. A. A. Sales and C. Airoidi, *J. Therm. Anal. Calorim.*, 2002, **70**, 191.
- 30 M. Klavins, L. Eglite and A. Zicmanis, *Chemosphere*, 2006, **62**, 1500.
- 31 C. Barbot, O. Bouloussa, W. Szymczak, M. Plaschke, G. Buckau, J.-P. Durand, J. Pieri, J. I. Kim and F. Goudard, *Colloids Surf., A*, 2007, **297**, 221.
- 32 R. S. Swift, in *Methods of soil analysis. Part 3. Chemical methods*, ed. D. L. Sparks, A. L. Page, P. A. Helmke, R. H. Loeppert, P. N. Soltanpour, M. A. Tabatabai, C. T. Johnson, and M. E. Sumner, SSSA Book Series 5. SSSA, Madison, WI, 2006, p. 1036.
- 33 I. V. Perminova, F. H. Frimmel, A. V. Kudryavtsev, N. A. Kulikova, G. Abbt-Braun, S. Hesse and V. S. Petrosyan, *Environ. Sci. Technol.*, 2003, **37**, 2477.
- 34 N. Hertkorn, A. B. Permin, I. V. P. erminova, D. V. Kovalevskii, M. V. Yudov and A. Kettrup, *J. Environ. Qual.*, 2002, **31**, 375.
- 35 J. H. Ng and L. L. Ilag, *Biotechnol. Annu. Rev.*, 2003, **9**, 1.
- 36 M. U. Kumke, F. H. Frimmel, F. Ariese and C. Gooijer, *Environ. Sci. Technol.*, 2000, **34**, 3818.
- 37 I. V. Perminova, N. Yu. Grechishcheva and V. S. Petrosyan, *Environ. Sci. Technol.*, 1999, **33**, 3781.
- 38 L. Abu-Lail L, Y. Liu, A. Atabek and T. A. Camesano, *Environ. Sci. Technol.*, 2007, **41**, 8031.
- 39 J. M. Gorham, J. D. Wnuk, M. Shin and H. Fairbrother, *Environ. Sci. Technol.*, 2007, **41**, 1238.
- 40 K. J. Wilkinson, E. Balnois, G. G. Leppard and J. Buffle, *Colloids Surf., A*, 1999, **155**, 287.
- 41 X. Ge, Y. Zhou, C. Lü and H. Tang, *Sci. China, Ser. B: Chem.*, 2006, **49**, 256.
- 42 A. G. Liu, *Colloids Surf., A*, 2000, **174**, 245.
- 43 P. Grathwohl and M. M. Rahman, *Isr. J. Chem.*, 2002, **42**, 67.